JOURNAL OF AERONAUTICS AND SPACE TECHNOLOGIES
JANUARY 2016 VOLUME 9 NUMBER 1 (1-13)

SATELLITE IMAGE PROCESSING WORKFLOW FOR RASAT AND GÖKTÜRK-2

Mustafa TEKE

TÜBİTAK UZAY Space Technologies Research Institute, Ankara - Turkey,
mustafa.teke@tubitak.gov.tr

Received: *02nd May 2014,* ***Accepted:*** *23rd July 2015*

ABSTRACT
We rely on Earth observation satellites to continuously observe the Earth. To be useful, raw images acquired by these satellites are processed in several levels. In this paper, automated satellite image processing operations for RASAT and Göktürk-2 images are described as a workflow. Automated satellite image processing operations include radiometric calibration, MTF sharpening, band registration, flare correction, georeferencing, orthorectification, pansharpening, colour enhancement and edge sharpening. Careful design and application of these steps are important to retain an acceptable level of radiometric and geometric accuracy as well as visual quality for use with various applications. Finally, we introduce our satellite image processing workflow with automated processing steps, so that human intervention will be minimum and there will be standard products free from human error.

Keywords*: RASAT, Göktürk-2, Satellite Image Processing, Registration, Radiometric Calibration, Georeferencing.*

RASAT VE GÖKTÜRK-2 İÇİN UYDU GÖRÜNTÜ İŞLEME İŞ AKIŞI

ÖZET
Dünyamızı sürekli gözlemlemek için yer gözlem uydularını kullanıyoruz. Yer gözlem uydularından alınan ham görüntülerin faydalı olabilmesi için, bu görüntüler çeşitli seviyelerde işlenmektedirler. Bu çalışmada, RASAT ve Göktürk-2 uydularının görüntülerinin işlenmesi için otomatik iş akışı tanımlanmaktadır. Önerilen otomatik iş akışı radyometrik kalibrasyon, MTF keskinleştirme, bant çakıştırma, parlama temizleme, jeoreferanslama, ortodüzeltme, pankeskinleştirme, renk iyileştirme ve kenar keskinleştirme işlemlerini içermektedir. Bu adımların, doğru tasarlanması ve uygulanması, farklı uygulamalar için yüksek radyometrik ve geometrik doğruluğa sahip görselliği yüksek görüntüler üretilmesi için gereklidir. Tanımlanan otomatik iş akışı sayesinde insan hatasından bağımsız standart uydu görüntüleme ürünleri oluşacaktır.

Anahtar Kelimeler: *RASAT, Göktürk-2, Uydu Görüntü İşleme, Çakıştırma, Radyometrik Kalibrasyon, Jeoreferanslama.*

1. INTRODUCTION

Available satellite imagery for commercial and public use are increasing incrementally as the number of earth observation satellites grow[1]. Satellite images are used in various fields including but not limited to urban planning, navigation, forestry, agriculture and geology. Spatial and spectral resolution requirements are unique for different areas; for example urban planning applications require higher spatial resolution than other fields. As of today 31 cm spatial resolution is commercially available with WorldView-3.

Most satellite systems have pushbroom sensors, which typically acquire a line for each band and these lines are collected to form discrete image bands. Satellite sensors often consist of one high resolution panchromatic sensor which have wider spectrum and smaller pixels. In most cases, there are also multispectral bands which collect light in narrower wavelength regions with 4 or 16 times larger pixels.

RASAT satellite is the first domestically built satellite of Turkey[2]. The aim was to independently design and build a remote sensing satellite, with a view to verify indigenous modules in space. Ground sampling distance (GSD) of RASAT is 7.5 m for pan and 15 m for RGB imager (Table 1). Since its launch on 17th August 2011, over 6 million km^2 imagery has been acquired by RASAT. It is currently operated by TÜBİTAK UZAY Space Technologies Research Institute RASAT images are available at GEZGİN Geoportal (www.gezgin.gov.tr).

Göktürk-2 is the second mini satellite of Turkey, which was built by TÜBİTAK UZAY and Turkish Aerospace Industries Inc. consortium. The Göktürk-2 spacecraft was launched on 18th December 2012. Göktürk-2 has significantly better spatial and spectral resolution than RASAT: 2.5 m for panchromatic band and 5 m for multispectral bands which include NIR in addition to the usual RGB (Table 1). While Göktürk-2 satellite is operated by Turkish Air Force (TUAF) it caters to national civilian and military imaging needs.

Table 1. RASAT and Göktürk-2 specifications.

	RASAT	Göktürk-2
Bands	Pan/RGB	Pan/RGB-NIR
Spatial Resolution	7.5 m / 15 m	2.5 m / 5 m
Revisit Time	2.5 days (Avg.)	2.5 days (Avg.)
Swath Width	30 km	20 km
Radiometric Resolution	8-bit	11-bit

Satellite imagery could only be useful if images are pre-processed; to this end, georeferencing, radiometric calibration, band registration, MTF sharpening and pansharpening are important steps. In this paper, relative radiometric calibration, MTF sharpening, band registration, pansharpening, colour enhancements, georeferencing and orthorectification of RASAT and Göktürk-2 satellite imagery are discussed.

2. IMAGE PROCESSING WORKFLOW

Earth observation satellites acquire raw imagery. Raw data (Level 0 / L0) is processed further to have correct geometric and radiometric values. RASAT and Göktürk-2 Imagery Levels are given in Table 2.

Table 2. TÜBİTAK UZAY satellite imagery levels.

Levels	Explanation
L0	Raw data
L1	Radiometric correction applied
L1R	Band registration completed
L1RB	Flare removal corrected (RASAT Only)
L2	Georeferenced images
L3	Orthorectified images
RGB	Red/Green/Blue images
Pansharp	Pansharpened, enhanced and sharpened images.

In our image processing workflow, raw satellite imagery is processed to correct for radiometric defects, to have correct geographic coordinates and, for applications that do not need radiometric accuracy, a sharp and clear image to facilitate visual inspection needs. In L1 processing, radiometric correction, band registration, MTF Sharpening are performed. Images are georeferenced in L2. L3 is where orthorectification with a digital elevation model (DEM) is completed (Figure 1).

2.1. Radiometric Calibration and Correction

Satellite imagery should be converted to radiance so that imagery will be usable in scientific applications. Absolute radiometric calibration aims to determine conversion from Digital Number (DN) values to Top of Atmosphere (ToA) radiance values. On the other hand, relative radiometric calibration aims to normalize pixels in push broom sensor to a reference value even when the sensor uses more than one set of electronics to process the raw sensor data.

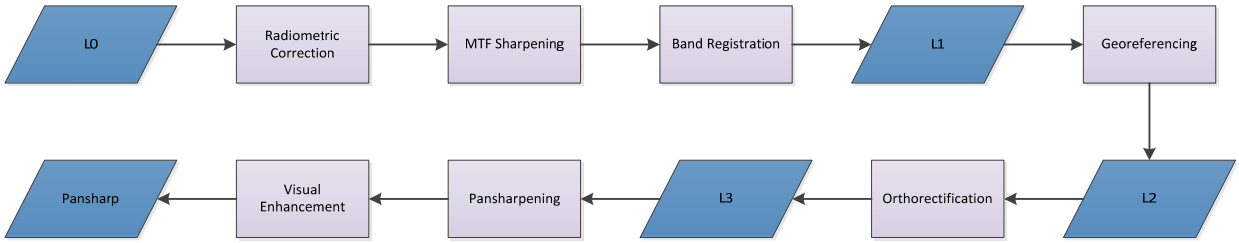

Figure 1. Imagery levels and processing steps.

Pre-flight sensor calibration is performed in laboratory tests before satellite integration. After the satellite is launched, on-orbit calibration is required: gain and offset parameters should be updated for each pixel. There are several instrumented absolute radiometric calibration and validation (cal/val) sites in

the world[3]. In Turkey, Tuz Gölü (Salt Lake) radiometric calibration site is used for absolute radiometric calibration which have uniform BRDF[4]. Such a calibration campaign requires a set of on-site measurements with simultaneous satellite imaging. On the other hand, Tuz Gölü is also only available in dry season (in August and September).

2.1.1. Cross Radiometric Calibration

Cross Radiometric Calibration is absolute radiometric calibration study which measures gain and offset parameters of a sensor from another calibrated sensor.

Landsat 8 satellite is used for cross radiometric calibration of Göktürk-2. Both satellites acquired images of Tuz Gölü on 29th August 2014 (Figure 2, Table 3). Göktürk-2 images are registered to Landsat-8 with nearest neighbour resampling to preserve spectral information.

Table 3. Göktürk-2 and Landsat 8 calibration images.

Satellite	Date	Time	Roll Angle	Sun Zenith	Sun Azimuth
Landsat 8	29/08/2014	10:27	0	34.65	142.61
Göktürk-2	29/08/2014	10:58	-3.71	38.38	132.87

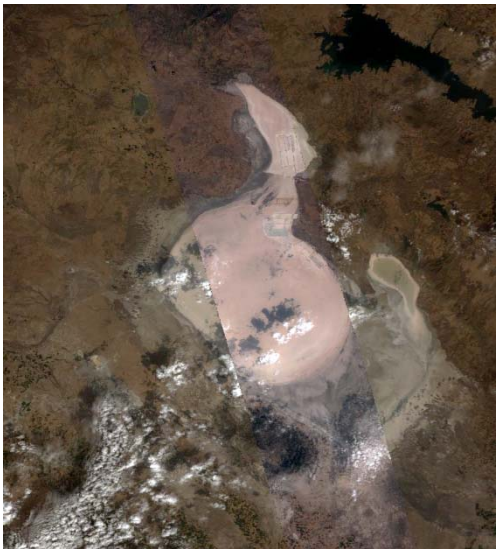

Figure 2. Salt Lake images of Landsat 8 (base image) and Göktürk-2.

ToA Reflectance is determined by the following formula:

$$\rho = \frac{\pi * L * d^2}{E_{SUN} * \cos\theta} \quad (1)$$

ρ: ToA Reflectance
L: Spectral Radiance ($L = Gain * DN + Offset$)
d: Earth-Sun distance in astronomical units
E_{SUN}: mean solar exoatmospheric irradiances
θ: Sun zenith angle (*zenith = 90 – elevation*)

Since reflectance of Salt Lake is invariant regardless of look angle and time difference between images is small the following equality is set:

$$\frac{L_{L8}}{E_{SUN_{L8}} * \cos\theta_{L8}} = \frac{L_{GK2}}{E_{SUN_{GK2}} * \cos\theta_{GK2}} \quad (2)$$

Then radiance of Göktürk-2 is then obtained as

$$L_{GK2} = L_{L8} * \frac{\cos\theta_{GK2}}{\cos\theta_{L8}} * \frac{E_{SUN_{GK2}}}{E_{SUN_{L8}}} \quad (3)$$

Several samples are collected from homogenous areas of Tuz Gölü to determine Gain and Offset values of each band. Gain and offset values of Göktürk-2 is given by Table 4. Spectral information and E_{SUN} values of Göktürk-2 are provided by Table 5.

Table 4. Gain and offset values of Göktürk-2.

	Pan	Red	Green	Blue	NIR
Gains	0.271358	0.193523	0.349076	0.268814	0.165102
Offsets	0	0	0	0	0

Table 5. Göktürk-2 spectral information.

Band	Wavelength (μm)	Center	FWHM (nm)	E_{SUN}
Blue	0.450 – 0.520	485	74.7	1979
Green	0.520 – 0.600	560	73.5	1857
Red	0.63 – 0.690	660	133.2	1558
NIR	0.760 - 0.900	830	117.1	1056.3
Pan	0.450 – 0.900	675	300	1499

As illumination change throughout the year and location different gain modes combinations could be used. Normalized gain gains are obtained dividing gains by gain value of gain mode (-2), then desired gain value is computed for respective gain modes(Table 6).

Table 6.Göktürk-2 gain modes.

Gain Mode	-2	0	2	4	6	8	10
Gain Multiplier	0.99	1.48	2	2.5	3	3.5	4

Error values are 0.8% for soil, 3.4% for vegetation and 2.3% at Tuz Gölü. Major reason for difference in vegetation is BRDF(Bi-directional Reflectance Distribution Function) effect that vegetation have different reflectance values depending on viewing angle.

Kalkan *et al* validated computed gain and offset values to compute NDVI obtaining 0.06 average difference over -1 and -1 (3%)[5].

2.1.2. Relative Radiometric Calibration

Relative calibration normalizes pixels in the push broom sensors (also called pixel response non-uniformity correction, PRNU). On-orbit relative calibration is performed by using flat or homogenous regions. In our studies, using Sahara desert images, relative radiometric calibration parameters are estimated. For relative radiometric calibration, 31.02° N, 2.23° E coordinates in Algeria are selected. It should also be noted that reflectance of deserts close to the Equator may cause saturations in sensors. As a result, deserts like Gobi may be preferable for calibration after spring equinox and before the summer solstice. During summer, deserts in southern hemisphere should be preferred. Poles might not always be an option for calibration as high reflectance from ice may saturate some bands and cloud cover is usually unfavourable.

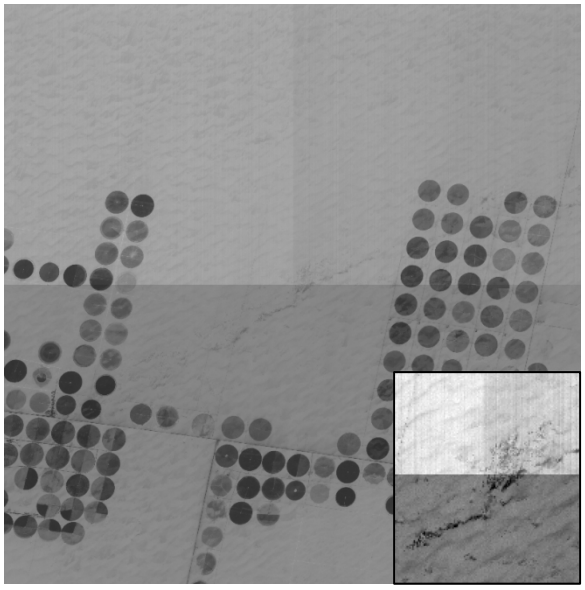

Figure 3. Result of relative radiometric correction: raw (upper part) and corrected (lower part). Center of the image is zoomed and contrast enhanced to strike pre and post calibration (lower right).

The algorithm for relative radiometric calibration is very simple and intuitive:

- Offset values are computed from each rows dark current pixels dynamically.
- Image of radiometric calibration site where the satellite is rotated 90°: so that every pixel in the sensor obtain image of same location.

Yaw 90° images are rotated 45° to find relative pixel responses. Computed pixel responses are applied to images along with dynamically computed offset values.

Results of the radiometric correction algorithm are displayed by Figure3.

2.2. MTF Sharpening

As satellite imagery is acquired, there are several factors which affect the quality of images: satellite motion, optical distortions and sensor quality[6]. In this section distortions from satellite motion and optics are considered and methods for correcting these distortions are provided.

As most Earth observation satellites orbit around the Earth at about 7 km/s and sensor scanning rates are not always very high, blurring effect occurs at pushbroom CCD sensors. Also the diffraction of light which is collected on a single pixel could be modelled as a PSF function. Türkmenoğlu and Yağlıoğlu conducted on-flight studies for RASAT satellite [7]. As for Göktürk-2 satellite a mathematical models are used for MTF (modulation transfer function) sharpening. MTF is also referred as optical transfer function (OTF). An ideal diffraction limited optical system tries to gather 83.8% of light to each pixel; as our sensors are push broom type imagers, PSF (point-spread function) filter in Figure 3 is obtained. Motion of the satellite is modelled with 6/8 of the light collected in the centre pixel. A combined filter which is displayed in Figure4 is used to sharpen images of Göktürk-2. Filter values are normalized 0-1 range to obtain sum of all values 1.

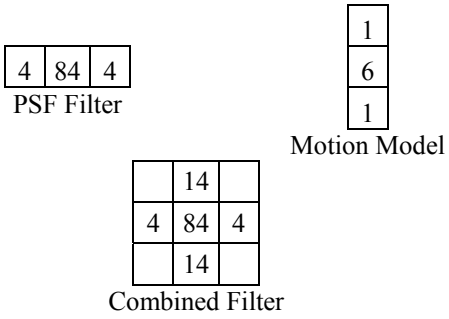

Figure 4. Preprocessing filters.

Lee *et al* use Richardson-Lucy deconvolution for MTF (modulation transfer function) sharpening of Kompsat-2 satellite images [8]. As the PSF is already known and amount of the noise is assumed to be very low, Wiener Deconvolution is used with our combined filter. Constrained least squared may also be used, however in our test the results were similar.

Results are shown in Figure5 where sharpening is evident in the MTF pattern from Salon de Provence, France.

A dedicated study for MTF sharpening should be conducted for precise sharpening of satellite imagery. After MTF is computed, PSF is obtained from MTF as MTF is Fourier Transform of PSF.

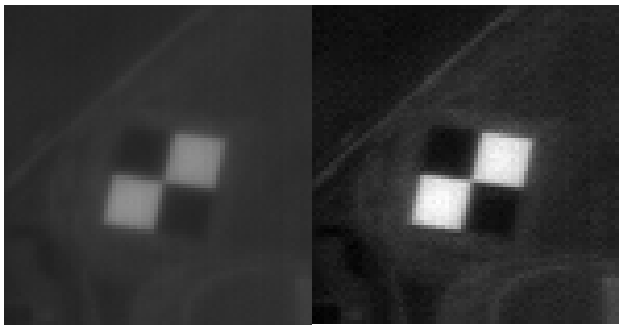

Figure 5. Göktürk-2 MTF sharpening original images (left), filtered images (right).

2.3. Band Registration

In addition to radiometric corrections and MTF sharpening, bands of Level 0 imagery are registered to obtain Level 1 imagery. In band registration, multispectral bands are co-registered to panchromatic band, and are often pansharpened to provide high resolution colour imagery with no geographic data. Push broom sensors acquire image of the same place in an order, while acquiring these lines the Earth also rotates. This causes shifts in cross track (x axis) of images.

Major approaches in image registration include feature descriptors based methods and correlation based methods [9]. Most commercial software use correlation based methods. Cross correlation and mutual information are commonly used examples of correlation based methods. Especially mutual information is very popular in medical image registration. RGB bands are in same modality as panchromatic band, however NIR band has different modality: for this reason Mattes' Mutual Information could be used to register images with different modalities [10]. SIFT and SURF are well known feature descriptors, they are widely used in image registration [11], [12]. In our tests, SIFT proved to be successful in detecting features even on regions where reflectance values are similar (for example no-vegetation areas) even if the number of matches is a fraction compared to RGB bands.

In our workflow, bands are registered using SIFT feature matching. A planar homography is assumed between image frames (32x32km^2 regions). As sensors of the different bands are physically very close (~100μm) to each other, it is safe to make this assumption. Band registration method detects features for each band. SIFT, SURF, ORB, FREAK features are evaluated. SIFT features are found to be most robust. However, for visible channel image matching other feature descriptors could also be used. Images are tiled for faster processing. For band registration, best features (usually 100 tie pointsare enough per megapixels) are selected. Also tiling enables parallel processing which result in speeding up computation.

For accurate matching nearest neighbour ratio is used, default value is 0.65 between first and second nearest neighbour. Registered points are further improved by eliminating outliers by RANSAC and a homography transform is computed between images. Multispectral bands are warped to panchromatic band with a second order polynomial transformation.

Test data is prepared by operators by using ERDAS LPS. For each band, test points in 256x256 sub windows are selected. For example for a single frame image (4096x4096) about 80 test points are selected per image.

Example shift values for RASAT and Göktürk-2 satellites are displayed in Table 7. RGB band values are similar for RASAT and Göktürk-2. NIR band only is available in Göktürk-2. NIR band of Göktürk-2 is placed in a different sensor group and has a significantly larger displacement than RGB bands to panchromatic band, as a result a large vertical shift exists for NIR. Matches between NIR and Pan bands are displayed in Figure 7.

Table 7. Example Shifts between bands for Göktürk-2 (in MS(multispectral) pixels).

	Horizontal Shift	**Vertical Shift**
Pan-Red	0.23	21.65
Pan-Green	0.36	30.78
Pan-Blue	0.39	12.79
Pan-NIR	82	1480

RASAT Pan-MS band registration values are around 0.8, and MS-MS band registration values are 0.4. Göktürk-2 has higher resolution and better registration performance (Table 8). Göktürk-2 Pan-MS band registration values for RGB bands are around 0.45 and Pan-NIR band registration error is 0.85 (Table 9). Registration results of MS Bands are shown on Figure 6.

Table 8. RASAT band registration results.

Band	RMSE (MS pixel)
Pan-Red	0.83
Pan-Green	0.78
Pan-Blue	0.82
Red-Green	0.41
Red-Blue	0.45

Table 9. Göktürk-2 band registration results.

Band	**RMSE (MS pixels)**
Pan-Red	0.45
Pan-Green	0.48
Pan-Blue	0.47
Pan-NIR	0.85

Our band registration results for Göktürk-2 is similar to WorldView-2 satellite. WV-2 has the following band registration accuracies: Pan-MS bands 1 Pan pixel, MS-MS (same group) bands under 0.5 Pan pixel, MS-MS (different group) just about 1 Pan pixel in CE90 (90% Circular Error) [13]. Since the NIR band of Göktürk-2 has a larger displacement, planar homography assumption does not work for rough surfaces. In this case, polynomial warping of NIR images should be applied.

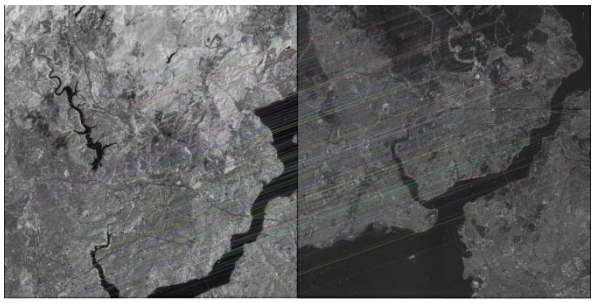

Figure 6. Matches between NIR and pan bands of Göktürk-2 imagery.

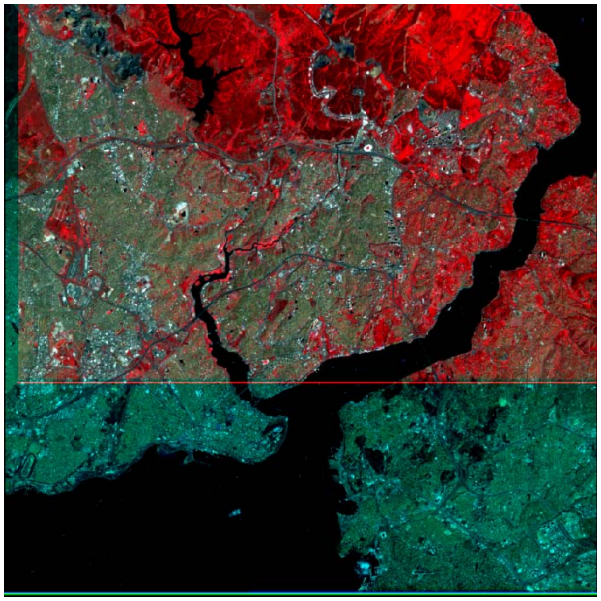

Figure 7. NIR false colour band registration result of Göktürk-2 imagery (red region shows overlapping areas NIR and other bands).

2.4. RASAT Red Band Flare Removal, Red Band Colour Balancing and Cloud Cover Computation

RASAT satellite's red band easily saturates even at the lowest sensor gain settings on bright and highly reflective regions (such as dry lands and deserts). Saturated pixels overflow to nearest pixels, this result in pixel loss. This effect will be called "flaring" for the remainder of this text.

Since, we use the knowledge that there is no natural bright red objects in scenes, values about certain threshold are considered as flares (>200). From a radiometric accuracy point of view, it is not possible to recover lost pixels. On the other hand, the ratio between pan, red, green and blue bands are approximated from several images. This prior information is used to estimate lost red band pixel values (1):

$$Red = (Pan - wG * Green - wB * Blue)/wR \quad (4)$$

where $wR = 0.22$, $wG = 0.32$, $wB = 0.12$ are respective band weights for Red, Green and Blue bands. These band weights values are experimentally determined from existing satellite images. Fixing red band flares is possible thanks to precise registration. There is a buffer zone around flare regions. Using morphological dilate operation, these buffer zones are also detected and restored. Results of flare removal operation are shown by Figure8.

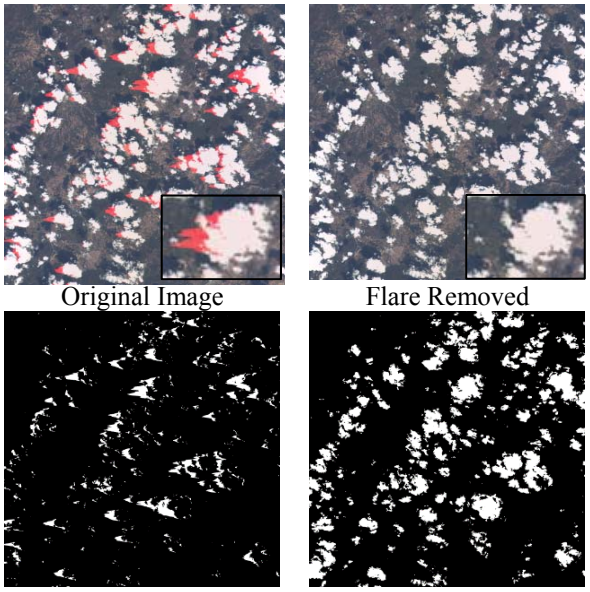

Figure 8. RASAT flare removal steps.

Similarly, as Red band collects more light, image colour balance is affected, causing a red tint in all images. Red channel colour is balanced using the channel weights which are given by (1).

Estimated Mean (μ_{est}) and variance (σ_{est}) of Red band is calculated using wR, wG and wB values and histogram of the red band is shifted using colour balancing according to (2)

$$RedCorrected = (Red - \mu_{Red}) * \sigma_{est}/\sigma_{Red} + \mu_{est} \quad (5)$$

The image in Figure9 has both flares and histogram shift in Red band, both of these problems are corrected.

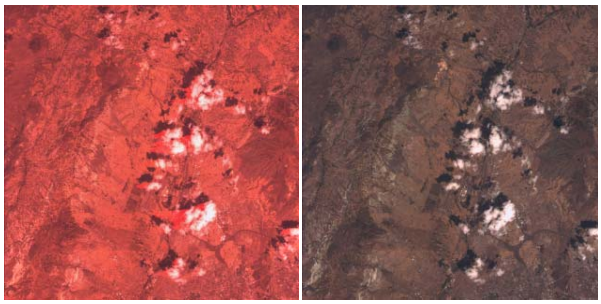

Figure 9. Saturated red band and corrected image.

Cloud cover information is another product that helps to quickly determine whether an image is usable or not. Clouds are fuzzy large white objects in satellite imagery and cloud regions are approximated by detecting regions where all bands have pixel values above a certain threshold, such as 225 or 235. There are methods which iteratively compute clouds [14] or NIR based methods [15], however simple thresholding over blue band gives an approximate cloud cover ratio. However snow regions result in false cloud detection results.

2.5. Georeferencing

Georeferencing of satellite images is one of the most important processing steps along with radiometric correction in satellite imagery applications as these application rely on high positional accuracy.

The standard method for georeferencing is to use actual or post-processed orbit and attitude information from the satellite and combine it with the sensor model to mark the location of each pixel on the ellipsoid. When more accurate reference data is available, Ground Control Points (GCPs) are used for highest positional accuracy.

As the star tracker on RASAT is not fully functional, the raw attitude data is not useful for high precision georeferencing. On the other hand, Göktürk-2 georeferenced image product has 100 meters or better accuracy. State of the art commercial satellites use much higher accuracy orbit and attitude sensors, leading to higher positional accuracies even without using GCPs, [13, 16](see Table 10).

Table 10. Georeferencing accuracy for commercial imaging satellites.

Satellite	Positional Accuracy (meters)
WorldView-1	3.6-4.9 [13]
WorldView-2	2.4-3.5 [13]
IKONOS	11.8[16]
QuickBird	14[16]
SPOT 6	19.3[17]
Pléiades 1B	8.5[17]

Regardless of the georeferencing accuracy obtained from the satellite, very high georeferencing accuracy requires corrections via GCPs whenever a prior reference data is available. Manual georeferencing is a time consuming task: for example the time required for orthorectifying 32x600 km^2 RASAT stripe is about 15 hours. Therefore, the next step is to find tie points from a reference and georeference images automatically and with no human intervention using a high accuracy reference data.

To this end, Landsat 8 panchromatic (Band 8, 15 m resolution) mosaic images of Turkey are used as a reference. Landsat 8 has 12 meter (CE90) positional accuracy [18]. Landsat 8 mosaic image is prepared to have minimal cloud cover using images obtained at different times of the year. Radiometrically corrected Landsat 8 reflectance image could also be used as a reference mosaic as images acquired at different times would be normalized to the similar reflectance values.

As RASAT images has low positional accuracy, an approximated area with a buffer is subset from Landsat 8 mosaic (around 5km). Reference Landsat 8 image is orthorectified, however RASAT image is in Cartesian coordinates. For this reason, it is not possible to completely register the image using planar assumption (i.e. planar geometry). Similar approach is georeferencing as in band registrations. Tie points from both images are computed using SIFT method. These tie points are matched with a ratio tests and are fitted to a 2^{nd} order polynomial geometry and an error threshold is applied to compensate local geometry changes.

RASAT images are warped using these tie points to increase positional accuracy from thousand meters to tens meters.

Göktürk-2 images are georeferenced in a similar fashion, but as the initial georeferencing information of much higher accuracy (on the order of 100 m) a narrower buffer region is deemed adequate.

Matches between RASAT's pan band (7.5 m) and Landsat 8 pan band (15 m) is shown byFigure10. An example of georeferenced Göktürk-2 image is shown by Figure 11.

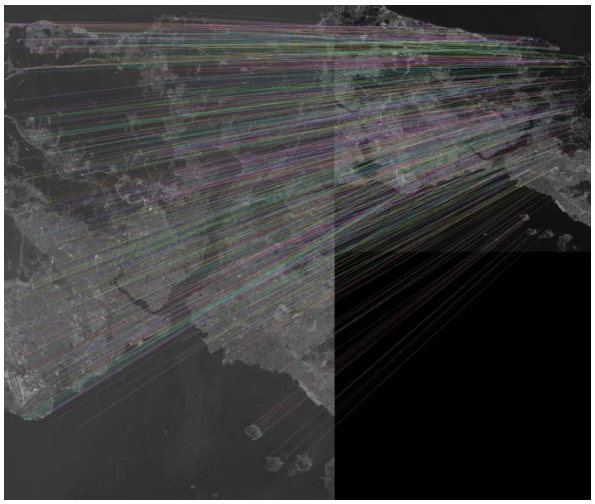

Figure 10. Matches between RASAT (left) and Landsat 8 (right) pan bands. Matches are shown as lines.

Figure 11. Georeferenced Göktürk-2 image (left) on Google Earth reference.

An example of georeferencing of RASAT images is shown by Figure 12. In our tests, we found out Göktürk-2 images has 10 meter registration accuracy by using Landsat-8 as a reference. This result is in accordance with the claimed positional accuracy of Landsat 8 images at 12 meter CE90 positional accuracy [18].

Orthorectified RASAT images have 20-30 meters positional errors while manually orthorectified Göktürk-2 images have 10-17 meters positional error values were computed in [19]. Different combinations of references (Landsat 8 and Google Earth), DEMs (SRTM, ASTER, DTED), and Number of GCPs for RASAT and Göktürk-2 are also presented [19]:the use of high resolution Google Earth reference had small effect for RASAT while Göktürk-2 georeferencing accuracy was increased noticeably compared to Landsat 8 reference.

Table 11 shows results of automatic image registration of 3 RASAT images with 8076 tie points with Landsat 8 reference image. 173 independent control points (ICP) are used to measure positional error. Tie point average error is fitting tie points to 3rd order polynomial model. Average error of 16.99 meter is better than manual registration performance where accuracy is lower than 20 meters. Because we do not use GCP points collected by using GNSS our results should be interpret as relative errors instead of absolute error.

Table 11. RASAT Georeferencing performance for ICPs.

Tie Point Avg Error (MS pixels)	ICP Avg Error (MS pixels)	ICP Avg Error (Meters)	ERDAS LPS ICP Avg Error (Meters)[19]
0.97	1.13	16.99	22.66

Major drawback of using a reference is the positional accuracy of the reference becomes the main source of error. Also obtaining references which are acquired at similar dates to satellite images is important for obtaining optimal registration results especially in agricultural and vegetation areas where land changes dynamically.

Landsat 8 data became available through cloud services such as Amazon's AWS cloud which makes it possible to access data through web for more accurate and easier reference access[20].

2.6. Orthorectification

For the orthorectification of RASAT imagery, there are two possible approaches: rational polynomial (RPC) based orthorectification and polynomial push broom camera model based orthorectification.

RPC parameters are preferred by satellite manufacturers as information regarding for mapping satellite imagery to earth coordinates are provided in the form of polynomials. As RASAT has no very precise georeferencing information, RPC parameters are computed by matching a reference mosaic (Landsat 8). At least 20 points are required to compute RPC parameters. However when there is a low number or poor distribution of matches, there may not always be a correct RPC solution.

If the sensor model of the satellite is known, polynomial push broom camera model could also be used. At the moment precise sensor models are still being studied, however it is possible to use ERDAS LPS/Photogrammetry software with matches from the georeferencing step.

A digital elevation model is used in the orthorectification process. SRTM data with 90 meter

spatial resolution is used as DEM. 30 meter SRTM-2 data will be globally available in 2015 [21].

RASAT and Göktürk-2 camera models are determined with pre-flight experiments in laboratory, however there will be studies to further improve accuracy via on-orbit determination of camera parameters.

Figure 12. Georeferencing of RASAT images of İzmir.

2.7. Visual Post Processing: Pansharp, Colour Enhancement and Sharpening

Panchromatic band of a satellite usually has a wider spectral coverage and has small physical pixel sizes. Individual multispectral bands have narrower spectral widths, and larger physical pixel sizes. Fusion of panchromatic images with low-resolution multispectral images is known as pansharpening.

An ideal pansharpening method preserves both spectral information of multispectral bands and spatial information of panchromatic band. In our studies, Hyperspherical Color Space (HCS) method [22] is selected as the pansharpening method [23], while HCS preserves colour best, edges are not as crisp as the result of Optimized High Pass Filter (HPF) [24] filter method. Pansharp methods are implemented in GPU allowing upto 20-30 times speed-up for RASAT images[25]. Visual comparison of HPF and HCS methods are displayed by Figure 13. Both of these methods are not limited to RGB channels unlike HSV method. Table 12 shows metric comparison of Gram-Schmidt (GS), HIS, Optimized HPF, HCS and Unsharp HCS. Unsharp (US) method is developed by TÜBİTAK UZAY where panchromatic band is sharpened with unsharp method before pansharpening operations. Metric results show that Optimized HPF provides similar RMSE of spectral bands as HCS while having higher spatial correlation to panchromatic band.

Table 12. Comparison of Pansharpening methods for Göktürk-2 images.

	GS	IHS	Opt HPF	HCS	US HCS
RMSE	53.87	49.60	**32.26**	**33.39**	46.87
Spatial	**0.96**	**0.97**	**0.97**	0.70	0.71

Figure 13. Comparison of HPF and HCS methods, RASAT image of Trabzon.

Raw satellite images have low dynamic ranges which have to be stretched for better colour and contrast reproduction. Also, as discussed in section 2.4,

RASAT Red band may in some cases be saturated, which results in unnatural images. Histogram Equalization, Min-Max stretching and Gaussian standard deviation stretching are well known contrast enhancement methods in remote sensing.

For RASAT and Göktürk-2 images, a hybrid contrast enhancement method is proposed: contrast limited adaptive histogram equalization (CLAHE, [26]) and Gaussian stretch are combined.

Our method is as follows:

1. Each band is stretched with CLAHE
2. 3σ (0.135% from bottom and 99.865%) values are computed from the histogram for each band.
3. Computed 3σ values are stretched to 1% to 95% (2-242) values so that dark and bright areas are not saturated.

2σ stretching is not preferred as darkest and brightest values are saturated in 0-255 range.

Final step in visual post processing is Unsharp masking. Contrary to its name, unsharp mask strengthens edges without amplifying noise using a threshold value. Edges are computed using a high pass filter, only strong edges are added to the original images which are above a threshold value. Unsharp mask method does not sharpen details in homogenous regions such as flat and featureless land and water bodies.

Combining these three steps, crisp and natural looking images are obtained. An example of all of these steps are applied to Göktürk-2 Ankara imagery is displayed in Figure 14. Visual post processing is important because, users often compare satellite imagery against Google Earth images in which images are heavily processed.

Suggested post processing method is

HCS Pansharpening → CLAHE+STD3 → Unsharp (6)

However if HPF pansharpening is used

HPF Pansharpening → CLAHE+STD3 (7)

should be applied as HPF Pansharpening already includes edge sharpening.

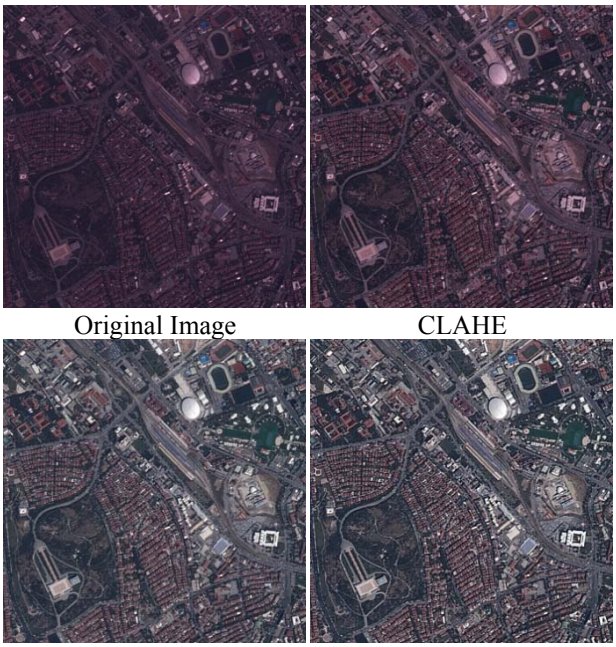

Original Image CLAHE

CLAHE+STD3 Stretch CLAHE+STD3+UnSharp

Figure 14. Comparison of post-processing stages, Anıtkabir, Atatürk's Mausoleum and Gençlik Parkı in Ankara, Göktürk-2 imagery.

CLAHE method improves images where mild haze exist; in this case, shifted up histogram of the scene is normalized. CLAHE method's dehaze performance is compared with RGB [27] and NIR [28] based methods; CLAHE provided better haze removal without degrading image.

Figure 15 shows a raw RASAT imagery and automatic processed imagery.

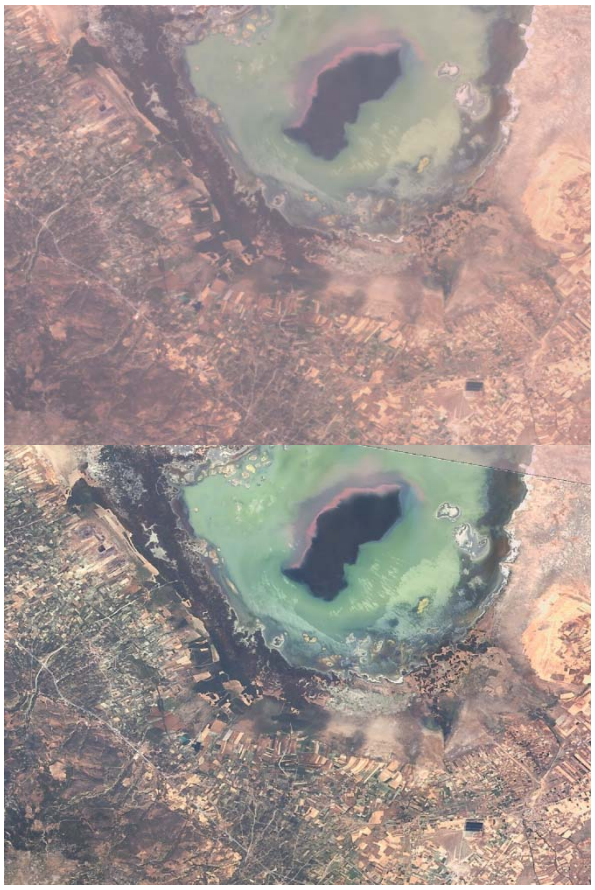

Figure 15. Results of image processing workflow defined in this study.

3. CONCLUSIONS AND FUTURE WORK

In this paper, satellite image processing workflow for RASAT and Göktürk-2 satellites has been described. Steps processing raw imagery to radiometrically corrected L1, geometrically corrected L2, and orthorectified L3 are defined. Pan sharpening and visual enhancements are described for both satellites.

Results of automatic image processing for RASAT are disseminated via GEZGİN Geoportal (https://www.gezgin.gov.tr) (Figure 16)[29]. As the number and the resolution of national satellites increase there will be a greater need for processing data accurately and efficiently. There should be detailed studies in big data from space: data should be processed in clusters and GPUs.

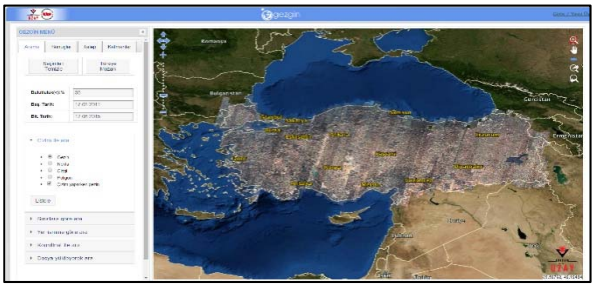

Figure 16. GEZGİN portal.

Defined workflow covers the most important requirements in satellite image processing. However the need still exists to develop solutions for DEM extraction from Stereo images and mosaic generation. There will be detailed studies in absolute calibration, geometric calibration and orthorectification. Also these processes in the workflow are continuously being improved.

A final note regarding multi-disciplinary nature of satellite image processing is that satellite image processing activities must be developed in conjunction with the development of the satellite. Also developing robust satellite image processing algorithms requires a basic understanding of satellite systems: one needs to have a fundamental knowledge in not only electro-optical sensor systems but also in attitude and orbit subsystems and how the data is processed.

Experience gained from developing image processing chains for RASAT and Göktürk-2 will benefit İMECE and MİYEG Projects. Also the experience will input design of future national earth observation satellites.

4. ACKNOWLEDGMENTS

I would like to thank Egemen İmre, Engin Tola and Sadık Murat Yüksel for their comments on the paper, Bülent Avenoğlu for giving opportunity on developing RASAT and Göktürk-2 image processing software, TÜBİTAK UZAY for providing RASAT satellite imagery and Turkish Air Force (TUAF) for providing Göktürk-2 satellite imagery.

5. REFERENCES

[1] A. S. Belward and J. O. Skoien, "Who launched what, when and why; trends in global land-cover observation capacity from civilian earth observation satellites," ISPRS Journal of Photogrammetry and Remote Sensing, vol. 103, no. May 2015, pp. 115-128, 2014.

[2] Ö. Kahraman, H. Özen, E. Demircioğlu, U. Sakarya, R. Küpçü, B. Avenoğlu, E. İmre and E. Bank, "Uzaktan algılamada RASAT: Türkiye'de üretilen ilk yer gözlem uydusu (RASAT in remote sensing: First earth observation satellite built in Turkey)," in IV. Uzaktan Algılama ve Coğrafi Bilgi Sistemleri Sempozyumu (UZAL-CBS 2012), Zonguldak, 2012.

[3] CEOS, "CEOS Cal/Val Portal," 2014. [Online]. Available: http://calvalportal.ceos.org/. [Accessed 23 April 2014].

[4] S. Gürol, H. Özen, U. Leloğlu and E. Tunalı, "Tuz Gölü: New absolute radiometric calibration test site," in ISPRS Congress, Beijing, China, 2008.

[5] K. Kalkan, Ö. Orhun, B. Filiz and M. Teke, "Vegetation Discrimination Analysis from Göktürk-

2," in Recent Advances in Space Technologies (RAST), 2015 7th International Conference on, 2015.

[6] U. Leloğlu and E. Tunalı, "On-orbit modulation transfer function estimation for BiLSAT imagers," in Proc. ISPRS, 2006.

[7] M. Türkmenoğlu and B. Yağlıoğlu, "On-orbit modulation transfer function estimation For RASAT," in Recent Advances in Space Technologies (RAST), 2013 6th International Conference on, 2013.

[8] J. Lee, J. Chun and D. Lee, "MTF compensation algorithm based on blind deconvolution for high-resolution remote sensing satellite," in SPIE Defense, Security, and Sensing, 2012.

[9] B. Zitová and J. Flusser, "Image registration methods: a survey," Image and Vision Computing, vol. 21, no. 11, pp. 977-1000, 2003.

[10] D. Mattes, D. R. Haynor, H. Vesselle, T. K. Lewellen and W. Eubank, "PET-CT image registration in the chest using free-form deformations," Medical Imaging, IEEE Transactions on, vol. 22, no. 1, pp. 120-128, 2003.

[11] M. Teke and A. Temizel, "Multi-spectral Satellite Image Registration Using Scale-Restricted SURF," in Pattern Recognition (ICPR), 2010 20th International Conference on, 2010.

[12] M. Teke, M. F. Vural, A. Temizel and Y. Yardımcı, "High-resolution multispectral satellite image matching using scale invariant feature transform and speeded up robust features," Journal of Applied Remote Sensing, vol. 5, no. 1, pp. 053553-053553-9, 2011.

[13] EOPortal, "Geolocation Accuracy of WorldView," 2014. [Online]. Available: https://directory.eoportal.org/web/eoportal/satellite-missions/v-w-x-y-z/worldview-2. [Accessed 19 April 2014].

[14] Q. Zhang and C. Xiao, Cloud Detection of RGB Color Aerial Photographs by Progressive Refinement Scheme, vol. PP, 2014, pp. 1-12.

[15] E. Baseski and C. Senaras, "Cloud detection in high-resolution satellite images," in Signal Processing and Communications Applications Conference (SIU), 2013 21st, 2013.

[16] R. Li, F. Zhou, X. Niu and K. Di, "Integration of IKONOS and QuickBird imagery for geopositioning accuracy analysis," Photogrammetric Engineering and Remote Sensing, vol. 73, no. 9, p. 1067, 2007.

[17] B. Cutler, "Pléiades 1B and SPOT 6 Image Quality status after commissioning and 1st year in orbit," in JACIE 2014 (Joint Agency Commercial Imagery Evaluation) Workshop, Louisville, Kentucky, USA, 2014.

[18] USGS, "Landsat 8," 2013. [Online]. Available: http://landsat.usgs.gov/landsat8.php. [Accessed 19 April 2014].

[19] R. Küpcü, M. Teke and A. Çabuk, "RASAT ve Göktürk-2 Görüntülerinin Ortorektifikasyon Başarımına Referans Ve Sayısal Yükseklik Modeli Seçiminin Etkisi," in V. Uzaktan Algılama ve Coğrafi Bilgi Sistemleri Sempozyumu (UZAL-CBS 2014), 2014.

[20] NASA, "More Ways to Get Landsat Data," [Online]. Available: http://landsat.gsfc.nasa.gov/?p=10221.

[21] JPL, "U.S. Releases Enhanced Shuttle Land Elevation Data," [Online]. Available: http://www.jpl.nasa.gov/news/news.php?release=2014-321.

[22] C. Padwick, M. Deskevich, F. Pacifici and S. Smallwood, "WorldView-2 pan-sharpening," Proc. American Society for Photogrammetry and Remote Sensing, p. 13, 2010.

[23] M. Teke, S. Seyfioğlu, A. Ağçal and S. Gürbüz, "Optimal Pansharpening of RASAT Satellite Imagery," in Signal Processing and Communications Applications Conference (SIU), 2014 22nd, 2014.

[24] U. G. Gangkofner, P. S. Pradhan and D. W. Holcomb, "Optimizing the high-pass filter addition technique for image fusion," Photogrammetric Engineering & Remote Sensing, vol. 74, no. 9, pp. 1107-1118, 2008.

[25] İ. Açıkgöz, M. Teke, U. Kutbay and F. Hardalaç, "Performance Evaluation of Pansharpening Methods on GPU for RASAT Images," in Recent Advances in Space Technologies (RAST), 2015 7th International Conference on, 2015.

[26] K. Zuiderveld, "Contrast limited adaptive histogram equalization," in Graphics gems IV, 1994.

[27] K. He, J. Sun and X. Tang, "Single Image Haze Removal Using Dark Channel Prior," Pattern Analysis and Machine Intelligence, IEEE Transactions on, vol. 33, no. 12, pp. 2341-2353, Dec 2011.

[28] C. Feng, S. Zhuo, X. Zhang, L. Shen and S. Susstrunk, "Near-infrared guided color image dehazing," in Image Processing (ICIP), 2013 20th IEEE International Conference on, 2013.

[29] M. Teke, T. Tevrizoğlu, A. Öztoprak, C. Demirkesen, İ. Açıkgöz, S. Gürbüz, R. Küpcü and B. Avenoğlu, "GEOPORTAL: TÜBİTAK UZAY Satellite Data Processing and Sharing System," in Recent Advances in Space Technologies (RAST), 2015 7th International Conference on, 2015.

VITAE

Mustafa TEKE

Mustafa Teke was born in Osmancık, Çorum in 1982. He graduated from Middle East Technical University (METU), Department of Electrical and Electronics Engineering in 2005. He received his M.S. degree from METU, Informatics Institute in 2010. He is currently a PhD student at Informatics Institute, METU. Since 2005, he has been working as software engineer in field of military defence sector with several companies. He is currently working as a researcher in Image Processing group of TÜBİTAK UZAY. His current research interests are in the field of remote sensing, signal and image processing, pattern recognition and computer vision especially in satellite image processing and hyperspectral image classification.